

## Majorana-Mediated Spin Transport in Kitaev Quantum Spin Liquids

Tetsuya Minakawa,<sup>1</sup> Yuta Murakami<sup>1</sup>,,<sup>1</sup> Akihisa Koga<sup>1</sup>,,<sup>1</sup> and Joji Nasu<sup>2,3</sup>

<sup>1</sup>*Department of Physics, Tokyo Institute of Technology, Meguro, Tokyo 152-8551, Japan*

<sup>2</sup>*Department of Physics, Yokohama National University, Hodogaya, Yokohama 240-8501, Japan*

<sup>3</sup>*PRESTO, Japan Science and Technology Agency, Honcho Kawaguchi, Saitama 332-0012, Japan*



(Received 18 December 2019; accepted 26 June 2020; published 24 July 2020)

We study the spin transport through the quantum spin liquid (QSL) by investigating the real-time and real-space dynamics of the Kitaev spin system with zigzag edges using the time-dependent Majorana mean-field theory. After the magnetic-field pulse is introduced to one of the edges, spin moments are excited in the opposite edge region although spin moments are never induced in the Kitaev QSL region. This unusual spin transport originates from the fact that the  $S = 1/2$  spins are fractionalized into the itinerant and localized Majorana fermions in the Kitaev system. Although both Majorana fermions are excited by the magnetic pulse, only the itinerant ones flow through the bulk regime without spin excitations, resulting in the spin transport in the Kitaev system despite the presence of a nonzero spin gap. We also demonstrate that this phenomenon can be observed in the system with small Heisenberg interactions using the exact diagonalization.

DOI: [10.1103/PhysRevLett.125.047204](https://doi.org/10.1103/PhysRevLett.125.047204)

Spin transport without an electric current has attracted not only practical interest in spintronics but also considerable attention in modern condensed matter physics. In insulating magnets, the carriers of the spin current are conventionally considered to be magnons, which are elementary excitations in a magnetically ordered state [1–4]. By contrast, the possibility of the spin transport in the quantum spin liquid (QSL) has been discussed recently [5,6]. One of the typical examples is an antiferromagnetic Heisenberg spin-1/2 chain, where elementary excitations are described by the spinon with an  $S = 1/2$  spin. The spin Seebeck experiments for the cuprate  $\text{Sr}_2\text{CuO}_3$ , a candidate material of the quasi-one-dimensional Heisenberg system, have clarified that the spin current is mediated by the spinons [6]. Therefore, the spinons, instead of the magnons, can be responsible for the spin transport in the nonmagnetic system.

Another interesting playground of the QSL is the Kitaev model [7], which has been studied intensively in this decade [8–35]. The Kitaev model consists of bond-dependent Ising interactions between spin-1/2 moments on a honeycomb lattice, and its ground state is exactly shown to be a QSL. One of the interesting features is the spin fractionalization. Namely, the spins are fractionalized into itinerant and localized Majorana fermions. Since both quasiparticles are charge neutral, the thermal transport is one of the most promising phenomena to grasp the presence of the Majorana fermions. In particular, in the Kitaev candidate material  $\alpha\text{-RuCl}_3$  [36–39], a half-integer quantized plateau in the thermal quantum Hall effects was observed [40], which is direct evidence of a topologically protected chiral Majorana edge mode. On the other hand, less is known about the spin

transport in the Kitaev QSL although it has recently been discussed in the related systems [41–43].

In the Kitaev model, the QSL has nonzero spin gap, and spin correlations are extremely short-ranged due to the existence of local  $Z_2$  symmetries, in contrast to the Heisenberg chain with power-law spin correlations. However, it does not necessarily mean the absence of the spin transport. When small local perturbations are present in the system, e.g., the magnetic field, edges, defects, etc., the  $Z_2$  symmetry is lost in certain regions [44]. Therefore, intriguing phenomena such as spin transport between these regions may be realized. It is highly desired to examine the spin transport in the nonequilibrium dynamics, which should be important to observe the itinerant nature of the Majorana fermions in the bulk.

In this Letter, to address the spin transport through the Kitaev QSL, we investigate the real-time dynamics triggered by a magnetic-field pulse on one of the edges. Using the time-dependent mean-field (MF) theory, we examine the time evolution of the magnetization and dynamics of the fractionalized Majorana quasiparticles. We demonstrate that a spin-polarized wave packet created at the edge propagates to the other edge even when the two edges are separated by the QSL region without spin polarization. We then clarify that the spin transport is mediated by the itinerant Majorana fermions. We also address how robust this anomalous phenomenon is against the Heisenberg interactions by means of the exact diagonalization (ED). Finally, we propose the ways to extract the results intrinsic to the Kitaev QSL with the fractionalized quasiparticles in experiments.

We consider the Kitaev model in the  $L_a \times L_b$  cluster of the honeycomb lattice with zigzag edges, which is

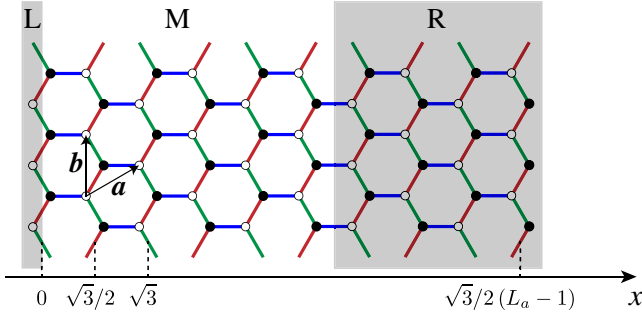


FIG. 1. Kitaev model on a honeycomb lattice with zigzag edges. Red, blue, and green lines represent  $x$ ,  $y$ , and  $z$  bonds, respectively. Solid (open) circles represent spin-1/2 in the  $A$  ( $B$ ) sublattice. In this figure, four  $z$  (green) bonds exist along the  $a$  direction in the  $R$  region, namely,  $L_R = 4$ .

schematically shown in Fig. 1. The norms of the primitive translational vectors  $\mathbf{a}$  and  $\mathbf{b}$  are assumed to be unity. The periodic boundary condition is imposed along the  $\mathbf{b}$  direction. The system that we consider here is composed of three regions. In the middle ( $M$ ) region, no magnetic field is applied and the Kitaev QSL is realized without spin polarization. In the right ( $R$ ) region, the static magnetic field  $h_R$  is applied. We introduce  $L_R$ , which is defined as the number of  $z$  bonds included in this region with respect to the  $\mathbf{a}$  direction (see Fig. 1). Moreover, we term the  $L$  region composed of the left-edge sites. In this region, we introduce the time-dependent magnetic field  $h_L(t)$ . The corresponding Hamiltonian is

$$\mathcal{H}(t) = -J_K \sum_{\gamma=x,y,z} \sum_{\langle i,j \rangle_{\gamma}} S_i^{\gamma} S_j^{\gamma} - h_R \sum_{i \in R} S_i^z - h_L(t) \sum_{i \in L} S_i^z, \quad (1)$$

where  $S_i^{\gamma}$  is the  $\gamma (= x, y, z)$  component of an  $S = 1/2$  spin operator at the  $i$ th site. The ferromagnetic exchange  $J_K (> 0)$  is defined on three different types of the nearest-neighbor bonds,  $x$  (red),  $y$  (blue), and  $z$  (green) bonds (see Fig. 1). It is known that, in the uniform lattice, the magnetic field induces the phase transition to the spin-polarized state [31,45–55]. The critical [001] field  $h_c$  has been evaluated as  $\sim 0.042J_K$  by the MF theory [31,52] and  $\sim 0.03J_K$  by the variational method [54]. Therefore, we restrict ourselves to the case with  $h_R < h_c$  to discuss the spin transport inherent in the Kitaev QSL.

We study the time evolution of the system upon stimuli of the magnetic pulse in the  $L$  region (see Fig. 1) [56,57]. To this end, we introduce the time-dependent Majorana MF theory [58]. The Hamiltonian given in Eq. (1) is rewritten as a fermion model by applying the Jordan-Wigner transformation to the spin operators [59–61]. Furthermore, by introducing two kinds of Majorana fermions,  $\gamma$  and  $\bar{\gamma}$ , from a complex fermion at each site, Eq. (1) is rewritten as

$$\begin{aligned} \mathcal{H}(t) = & -\frac{J_K}{4} \sum_{\mathbf{r}} (i\gamma_{\mathbf{r}-\mathbf{a}+\mathbf{b}}^A \gamma_{\mathbf{r}}^B + i\gamma_{\mathbf{r}+\mathbf{b}}^A \gamma_{\mathbf{r}}^B) \\ & -\frac{J_K}{4} \sum_{\mathbf{r}} i\gamma_{\mathbf{r}}^A \gamma_{\mathbf{r}}^B i\bar{\gamma}_{\mathbf{r}}^A \bar{\gamma}_{\mathbf{r}}^B \\ & -\frac{h_R}{2} \sum_{\mathbf{r} \in R} (i\gamma_{\mathbf{r}}^A \bar{\gamma}_{\mathbf{r}}^A - i\gamma_{\mathbf{r}}^B \bar{\gamma}_{\mathbf{r}}^B) + \frac{h_L(t)}{2} \sum_{\mathbf{r} \in L} i\gamma_{\mathbf{r}}^B \bar{\gamma}_{\mathbf{r}}^B, \quad (2) \end{aligned}$$

where  $\mathbf{r}$  indicates the position of the  $z$  bond (the center of the  $z$  bond, see Fig. 1).  $\gamma_{\mathbf{r}}^A$  and  $\bar{\gamma}_{\mathbf{r}}^A$  ( $\gamma_{\mathbf{r}}^B$  and  $\bar{\gamma}_{\mathbf{r}}^B$ ) are the Majorana fermion operators connected with the  $z$  bond in the sublattice  $A$  ( $B$ ), as shown in Fig. 1. When  $h_R = h_L(t) = 0$ ,  $[\mathcal{H}, \eta_{\mathbf{r}}] = 0$  at each  $\mathbf{r}$ , and  $\eta_{\mathbf{r}} (= i\bar{\gamma}_{\mathbf{r}}^A \gamma_{\mathbf{r}}^B)$  is the  $Z_2$  local conserved quantity. In the case, the model is solvable as the Hamiltonian is bilinear in terms of  $\gamma$ , and its low-energy dispersion is given as  $\varepsilon_{\mathbf{k}} \simeq v|\mathbf{k} - \mathbf{k}_K|$  around the  $K$  point with the velocity  $v = \sqrt{3}J_K/4$ . This indicates that  $\gamma$  and  $\bar{\gamma}$  are regarded as the itinerant and localized Majorana fermions, respectively.

Since the magnetic field hybridizes two kinds of the Majorana fermions, the Hamiltonian is no longer exactly solvable. Here, we apply the Hartree-Fock type decoupling to the interaction on the  $z$  bond as  $i\gamma_{\mathbf{r}}^A \gamma_{\mathbf{r}}^B \times i\bar{\gamma}_{\mathbf{r}}^A \bar{\gamma}_{\mathbf{r}}^B \sim i\gamma_{\mathbf{r}}^A \gamma_{\mathbf{r}}^B \Theta_1(x, t) + \Theta_2(x, t) i\bar{\gamma}_{\mathbf{r}}^A \bar{\gamma}_{\mathbf{r}}^B - \Theta_1(x, t) \Theta_2(x, t) - i\gamma_{\mathbf{r}}^A \bar{\gamma}_{\mathbf{r}}^A \Theta_3(x, t) - \Theta_4(x, t) i\gamma_{\mathbf{r}}^B \bar{\gamma}_{\mathbf{r}}^B + \Theta_3(x, t) \Theta_4(x, t) - i\gamma_{\mathbf{r}}^A \bar{\gamma}_{\mathbf{r}}^B \times \Theta_5(x, t) - \Theta_6(x, t) i\bar{\gamma}_{\mathbf{r}}^A \gamma_{\mathbf{r}}^B + \Theta_5(x, t) \Theta_6(x, t)$ , where we have introduced the six kinds of  $x$ - and  $t$ -dependent MFs as  $\Theta_1(x, t) = \langle i\bar{\gamma}_{\mathbf{r}}^A \bar{\gamma}_{\mathbf{r}}^B \rangle \equiv \langle \eta \rangle(x, t)$ ,  $\Theta_2(x, t) = \langle i\gamma_{\mathbf{r}}^A \gamma_{\mathbf{r}}^B \rangle \equiv \langle \xi \rangle(x, t)$ ,  $\Theta_3(x, t) = \langle i\gamma_{\mathbf{r}}^B \bar{\gamma}_{\mathbf{r}}^B \rangle = -2\langle S_B^z \rangle(x, t) = -2\langle S^z \rangle(x - x_d/2, t)$ ,  $\Theta_4(x, t) = \langle i\gamma_{\mathbf{r}}^A \bar{\gamma}_{\mathbf{r}}^A \rangle = 2\langle S_A^z \rangle(x, t) = 2\langle S^z \rangle(x + x_d/2, t)$ ,  $\Theta_5(x, t) = \langle i\bar{\gamma}_{\mathbf{r}}^A \gamma_{\mathbf{r}}^B \rangle$ ,  $\Theta_6(x, t) = \langle i\gamma_{\mathbf{r}}^A \bar{\gamma}_{\mathbf{r}}^B \rangle$ , where  $x$  is the horizontal coordinate of  $\mathbf{r}$  and  $x_d = 1/(2\sqrt{3})$ . This MF theory is exact when  $h_L = h_R = 0$ . Therefore, we believe that our MF results are reliable as far as the small fields are applied. In the MF theory, the many-body wave function is expressed as a direct product of one-body states, whose time-evolution is described by the MF Hamiltonian. Determining the MFs at each time from the many-body wave function, we compute the time evolution of the one-body states with the extended Euler method [62–67]. The time-dependent magnetic field is explicitly given as,  $h_L(t) = (A/\sqrt{2\pi}\sigma) \exp[-(t^2/2\sigma^2)]$ , where  $A$  and  $\sigma$  are constants for the Gaussian pulse. In the following, we fix the system size as  $L_a = 50$  and  $L_b = 300$ , the static field as  $h_R = 0.01J_K$ , and pulse parameters as  $A = 1$  and  $\sigma = 2J_K^{-1}$ .

Before discussing the spin transport through the  $M$  region, we examine the system without this region, namely, the static magnetic field  $h_R$  is applied to the sites in the  $R$  region with  $L_R = L_a - 1$ . In this case, there are no local conserved quantities, which does not prohibit the appearance of the local spin moments. Figure 2(a) shows the contour plot of the changes in the spin moments  $\Delta S^z(x, t)$ , where  $\Delta O(x, t) = \langle O(x, t) \rangle - \langle O(x, -\infty) \rangle$ . As expected, we find that the wave packet created by the magnetic-field

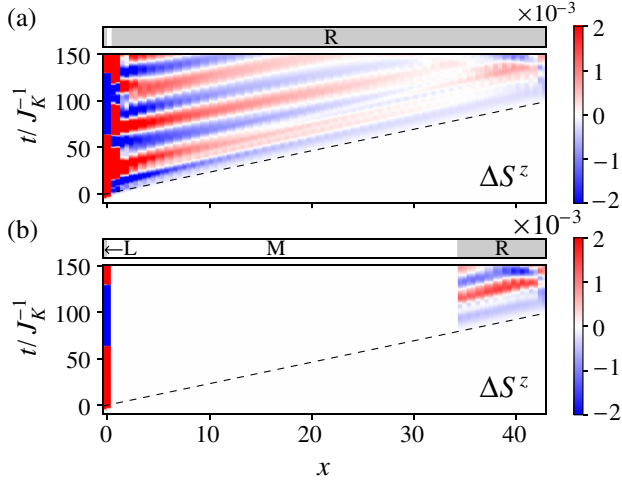


FIG. 2. Real-time dynamics of the Kitaev spin system with  $L_a = 50$  and  $L_b = 300$ . The contour plot of  $\Delta S^z(x, t)$  on the plane of the time  $t$  and the space  $x$  in the system (a) without and (b) with the M (white) region where the QSL is realized without spin polarization between the L (left gray) and R (right gray) regions (see the top of the panels). The dashed lines represent  $x = vt$  with the Majorana velocity  $v$  (see text).

pulse flows to the right edge. Note that its velocity almost coincides with the Majorana velocity of the genuine Kitaev model,  $v$ , which is shown as the dashed line in Fig. 2(a). This indicates that the propagation is attributed to the gapless Majorana excitation in the bulk within a small static field.

Now, we consider the real-time dynamics of the non-magnetic Kitaev spin system triggered by the magnetic-field pulse at the left edge to discuss how the wave packet flows through the M region (the Kitaev QSL with the local  $Z_2$  symmetry). In this region, the local conserved quantity is present in each hexagon, and spin correlations are extremely short ranged [68]. Figure 2(b) shows the time evolution of  $\Delta S^z(x, t)$  in the system with  $L_R = 10$ . We find that the magnetic moment is always zero in the M region and no proximity effect is found around the interface between L and M regions. Nevertheless, in the R region,  $\Delta S^z(x, t)$  is induced and the wave packet flows with the Majorana velocity  $v$ . This result indicates that the spin excitations propagate in the nonmagnetic region via the itinerant Majorana fermions, which cannot be explained by classical pictures such as the spin-wave theory.

To discuss the propagation of the spin excitation through the QSL region in more detail, we examine the time evolutions of  $\Delta\xi$  and  $\Delta\eta$ , which correspond to the dynamics of itinerant and localized Majorana fermions, as shown in Figs. 3(a) and 3(b). We find in Fig. 3(a) that the excitation created in the left edge at  $t = 0$  propagates in the whole region, which results from the motion of the itinerant Majorana fermions. By contrast, Fig. 3(b) shows that  $\Delta\eta$  vanishes in the M region owing to the existence of

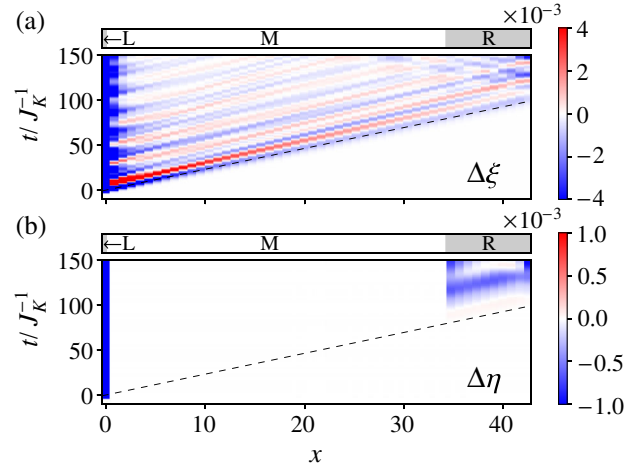


FIG. 3. Real-time evolution of (a)  $\Delta\xi$  and (b)  $\Delta\eta$  of the Kitaev spin system with  $L_a = 50$  and  $L_b = 300$ . The setup and parameters are the same as in Fig. 2(b).

the local  $Z_2$  symmetry, while it appears in the R region, as in  $\Delta S^z$ . These suggest that, after the excitation at the left edge, only the itinerant Majorana fermions propagate in the bulk without the magnetization being induced, and finally reach the R region. The weak magnetic field in the R region yields the hybridization between itinerant and localized Majorana fermions, resulting in time-dependent nonzero spin moments there. Thus, in the Kitaev QSL, the spin transport is mediated by the Majorana fermions although the spin moments never appear. Moreover, we have confirmed that the magnitude of the spin moment induced in the R region exhibits a power-law decay as a function of the length of the M region. This is ascribed to the gapless dispersion of the itinerant Majorana fermions, in contrast to the existence of the gap in the spin excitation in the Kitaev model. Note that the interesting transport properties found here are also observed in the system with armchair edges or other pulse parameters, which suggests that they are independent of the boundary or pulse conditions (see the Supplemental Material [69]). This is expected from the itinerancy of the Majorana fermions in all directions.

The pulse-amplitude dependence in this phenomenon is also remarkable. In the R region,  $\Delta S^z$  turns out to be proportional to  $A^2$  in the limit  $A \rightarrow 0$  [69]. This can be explained by considering the local symmetry at the left edge [70]. This nonlinear feature is intrinsic in the Kitaev model, in contrast to the conventional systems with  $\Delta S^z \propto A$ . To study how visible anomalous behavior is in the system with the Heisenberg interaction, we apply the ED method to the Hamiltonian  $\mathcal{H}(t) + J_H \sum_{\langle i,j \rangle} \mathbf{S}_i \cdot \mathbf{S}_j$  with the antiferromagnetic Heisenberg coupling  $J_H (> 0)$ . It is known that, when  $h_R = h_L(t) = 0$ , the Kitaev QSL is stable against small  $J_H$  [10,13,20,26]. In our calculations, the initial ground state is obtained with the Lanczos method and the time evolution is evaluated by the Runge-Kutta method.

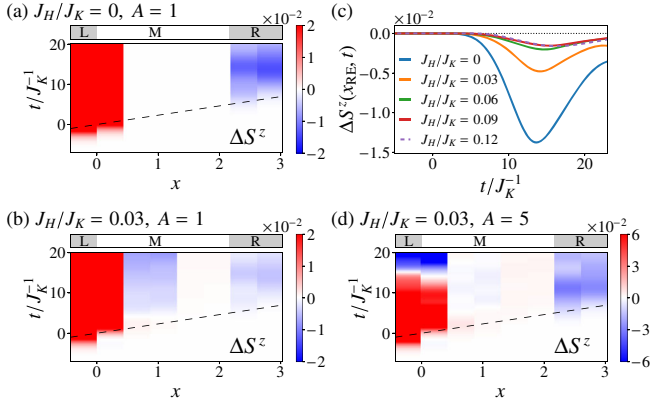


FIG. 4. Contour plots of  $\Delta S^z(x, t)$  in the 24-site cluster with  $h_R = 0.01J_K$  when (a)  $(J_H/J_K, A) = (0, 1)$ , (b)  $(0.03, 1)$ , and (d)  $(0.03, 5)$ . The dashed lines represent  $x = vt$  with the Majorana velocity  $v$  (see text). (c) Time evolution of  $\Delta S^z$  at the right edge site  $x_{RE}$  with  $A = 1$ .

The results for the 24-site cluster with  $L_a = 4$ ,  $L_b = 3$ , and  $L_R = 1$  are shown in Fig. 4. In the calculations, we have confirmed that the induced moment is always parallel to the  $z$  direction. First, we show the result for the genuine Kitaev model with  $J_H = 0$  in Fig. 4(a). One can find the propagation of the magnetic excitation from one edge to the other through the QSL region with the local  $Z_2$  symmetry, which is consistent with the MF result shown in Fig. 2(b). The reproducibility in the small cluster is ascribed to the quick damping of spin correlations in the M region, which clearly separates the two edge regions. This feature is also expected in the case with small additional interactions. In the presence of the Heisenberg term ( $J_H/J_K = 0.03$ ),  $\Delta S^z$  takes nonzero values in the M region, as shown in Fig. 4(b), which suggests that the Heisenberg interaction affects the flow of the spin excitation. In particular, the spin modulation in the left side of the M region is more prominent compared to that in the R region. This difference from the genuine Kitaev model originates from the fact that the Heisenberg interaction yields the interaction between itinerant and localized Majorana fermions. Therefore, the spin moments appear in the M region near the interface to the L region as a proximity effect.

To discuss the effect of the Heisenberg interaction, we show the time evolution of  $\Delta S^z$  at the right edge site  $x_{RE}$  in Fig. 4(c). The peak feature survives and the position of the first peak hardly changes in the small  $J_H$  cases. Since the peak position indicates the elapsed time from the creation of the spin wave packet at the left edge, the results imply that the velocity of the spin transport is mainly determined by the itinerant Majorana fermion even in the presence of small  $J_H$ . These suggest that the spin transport in the systems with small  $J_H$  reflects an intrinsic nature of the Kitaev QSL. On the other hand, the peak structure is strongly suppressed and its position is shifted above  $J_H/J_K \sim 0.1$ , which is consistent with the fact that the

Kitaev QSL becomes unstable [10,13,20,26]. However, more detailed investigations with larger-size clusters are needed around  $J_H/J_K \sim 0.13$  at which the Kitaev QSL changes to a magnetic ordered state. This will be for a future work to investigate.

When the pulse amplitude  $A$  is relatively large, the Kitaev interaction plays a dominant role for the spin propagation and the spin transport without spin polarization becomes practically prominent. Figure 4(d) presents the results with the large  $A$ . The spin moments induced in the M region are relatively small, but the spin excitation propagates to the right edge, at which the spin moments induced are much larger than those in the M region. This phenomenon is essentially the same as that in the genuine Kitaev case shown in Fig. 4(a).

Finally, we discuss the relevance of the present results to real materials. The setup of our study could be implemented by considering a Kitaev candidate material sandwiched by ferromagnetic insulators. The candidate materials have been proposed as  $A_2\text{IrO}_3$  ( $A = \text{Na, Li}$ ) [71–76] and  $\alpha\text{-RuCl}_3$  [36–39]. The stimuli of the magnetic field pulse can be injected from a ferromagnetic insulator by the spin pumping [77–80] or circular polarized light irradiation [81,82]. Our results suggest that the spin-excited flow propagates to the other edge even if the magnetic polarization is absent in the Kitaev magnet, and therefore we expect that the time-dependent magnetic moment is observed in the ferromagnetic insulator connected to the other side of the Kitaev magnet with a small overlapping. This time evolution can be experimentally measured by the Kerr or Faraday rotations [81,83], which will provide convincing evidence of the fractionalized itinerant quasi-particles in the bulk of the Kitaev magnet. Note that in the real system, a magnetic order hinders the appearance of the Kitaev QSL [84–89]. However, one may use the recent progress of the thin film [14,90–98], which suppresses the magnetic ordering due to the reduced interlayer coupling. The effect of the off-diagonal interactions, so-called  $\Gamma$  term, is not addressed in the present study but we expect that this gives a similar effect to the Heisenberg one [53,99,100].

In summary, we have demonstrated that the spin transport through the Kitaev QSL is mediated by the fractionalized itinerant Majorana fermions although spin moments are never induced in the bulk due to the local  $Z_2$  symmetry. Despite the presence of the nonzero spin gap, spin excitations propagate in the Kitaev QSL via gapless itinerant Majorana fermions, which is distinct from the spin transport in QSLs with spinon Fermi surfaces [5]. The Majorana-mediated spin transport should be visible even in the system with the Heisenberg coupling by using the pulse field dependence in  $\Delta S^z$ .

We note that it might be possible to control the motion of the localized Majorana fermions (vison) in the bulk by switching the magnetic field on and off. This should be important for realizing the vison transport in the



experiments. It is also interesting to study the spin transport in the generalized Kitaev models [101–104], where the existence of spin fractionalization has been suggested [102,105,106] to clarify the presence of quasiparticles.

The authors thank T. Mizoguchi and M. Udagawa for fruitful discussions. Parts of the numerical calculations were performed in the supercomputing systems in ISSP, the University of Tokyo. This work was supported by Grant-in-Aid for Scientific Research from JSPS, KAKENHI Grants No. JP19K23425 (Y.M.), No. JP17K05536, No. JP18K04678, No. JP19H05821 (A.K.), No. JP16H02206, No. JP18H04223, No. JP19K03742 (J.N.), by JST CREST (JPMJCR1901) (Y.M.), and by JST PREST (JPMJPR19L5) (J.N.).

- 
- [1] K.-i. Uchida, H. Adachi, T. Ota, H. Nakayama, S. Maekawa, and E. Saitoh, *Appl. Phys. Lett.* **97**, 172505 (2010).
- [2] K.-i. Uchida, J. Xiao, H. Adachi, J.-i. Ohe, S. Takahashi, J. Ieda, T. Ota, Y. Kajiwara, H. Umezawa, H. Kawai *et al.*, *Nat. Mater.* **9**, 894 (2010).
- [3] J. Xiao, G. E. W. Bauer, K.-c. Uchida, E. Saitoh, and S. Maekawa, *Phys. Rev. B* **81**, 214418 (2010).
- [4] S. M. Rezende, R. L. Rodríguez-Suárez, R. O. Cunha, A. R. Rodrigues, F. L. A. Machado, G. A. F. Guerra, J. C. L. Ortiz, and A. Azevedo, *Phys. Rev. B* **89**, 014416 (2014).
- [5] C.-Z. Chen, Q.-F. Sun, F. Wang, and X. C. Xie, *Phys. Rev. B* **88**, 041405(R) (2013).
- [6] D. Hirobe, M. Sato, T. Kawamata, Y. Shiomi, K.-i. Uchida, R. Iguchi, Y. Koike, S. Maekawa, and E. Saitoh, *Nat. Phys.* **13**, 30 (2017).
- [7] A. Kitaev, *Ann. Phys. (Amsterdam)* **321**, 2 (2006).
- [8] S. Dusuel, K. P. Schmidt, and J. Vidal, *Phys. Rev. Lett.* **100**, 177204 (2008).
- [9] G. Jackeli and G. Khaliullin, *Phys. Rev. Lett.* **102**, 017205 (2009).
- [10] J. Chaloupka, G. Jackeli, and G. Khaliullin, *Phys. Rev. Lett.* **105**, 027204 (2010).
- [11] K. Dhochak, R. Shankar, and V. Tripathi, *Phys. Rev. Lett.* **105**, 117201 (2010).
- [12] F. L. Pedrocchi, S. Chesi, and D. Loss, *Phys. Rev. B* **84**, 165414 (2011).
- [13] J. Chaloupka, G. Jackeli, and G. Khaliullin, *Phys. Rev. Lett.* **110**, 097204 (2013).
- [14] Y. Yamaji, Y. Nomura, M. Kurita, R. Arita, and M. Imada, *Phys. Rev. Lett.* **113**, 107201 (2014).
- [15] J. Nasu, M. Udagawa, and Y. Motome, *Phys. Rev. B* **92**, 115122 (2015).
- [16] Z. Nussinov and J. van den Brink, *Rev. Mod. Phys.* **87**, 1 (2015).
- [17] T. Suzuki, T. Yamada, Y. Yamaji, and S.-i. Suga, *Phys. Rev. B* **92**, 184411 (2015).
- [18] M. Schmitt and S. Kehrein, *Phys. Rev. B* **92**, 075114 (2015).
- [19] I. Rousochatzakis, J. Reuther, R. Thomale, S. Rachel, and N. B. Perkins, *Phys. Rev. X* **5**, 041035 (2015).
- [20] Y. Yamaji, T. Suzuki, T. Yamada, S.-i. Suga, N. Kawashima, and M. Imada, *Phys. Rev. B* **93**, 174425 (2016).
- [21] L. Janssen, E. C. Andrade, and M. Vojta, *Phys. Rev. Lett.* **117**, 277202 (2016).
- [22] X.-Y. Song, Y.-Z. You, and L. Balents, *Phys. Rev. Lett.* **117**, 037209 (2016).
- [23] R. Yadav, N. A. Bogdanov, V. M. Katukuri, S. Nishimoto, J. Van Den Brink, and L. Hozoi, *Sci. Rep.* **6**, 37925 (2016).
- [24] S. Trebst, [arXiv:1701.07056](https://arxiv.org/abs/1701.07056).
- [25] S. M. Winter, A. A. Tsirlin, M. Daghofer, J. van den Brink, Y. Singh, P. Gegenwart, and R. Valentí, *J. Phys. Condens. Matter* **29**, 493002 (2017).
- [26] M. Gohlke, R. Verresen, R. Moessner, and F. Pollmann, *Phys. Rev. Lett.* **119**, 157203 (2017).
- [27] J. Nasu, J. Yoshitake, and Y. Motome, *Phys. Rev. Lett.* **119**, 127204 (2017).
- [28] M. Hermanns, I. Kimchi, and J. Knolle, *Annu. Rev. Condens. Matter Phys.* **9**, 17 (2018).
- [29] H. Tomishige, J. Nasu, and A. Koga, *Phys. Rev. B* **97**, 094403 (2018).
- [30] A. Koga, S. Nakauchi, and J. Nasu, *Phys. Rev. B* **97**, 094427 (2018).
- [31] J. Nasu, Y. Kato, Y. Kamiya, and Y. Motome, *Phys. Rev. B* **98**, 060416(R) (2018).
- [32] J. Knolle and R. Moessner, *Annu. Rev. Condens. Matter Phys.* **10**, 451 (2019).
- [33] H. Takagi, T. Takayama, G. Jackelli, G. Khaliullin, and S. Nagler, *Nat. Rev. Phys.* **1**, 264 (2019).
- [34] H.-Y. Lee, R. Kaneko, T. Okubo, and N. Kawashima, *Phys. Rev. Lett.* **123**, 087203 (2019).
- [35] Y. Motome and J. Nasu, *J. Phys. Soc. Jpn.* **89**, 012002 (2020).
- [36] K. W. Plumb, J. P. Clancy, L. J. Sandilands, V. V. Shankar, Y. F. Hu, K. S. Burch, H.-Y. Kee, and Y.-J. Kim, *Phys. Rev. B* **90**, 041112(R) (2014).
- [37] Y. Kubota, H. Tanaka, T. Ono, Y. Narumi, and K. Kindo, *Phys. Rev. B* **91**, 094422 (2015).
- [38] J. A. Sears, M. Songvilay, K. W. Plumb, J. P. Clancy, Y. Qiu, Y. Zhao, D. Parshall, and Y.-J. Kim, *Phys. Rev. B* **91**, 144420 (2015).
- [39] M. Majumder, M. Schmidt, H. Rosner, A. A. Tsirlin, H. Yasuoka, and M. Baenitz, *Phys. Rev. B* **91**, 180401(R) (2015).
- [40] Y. Kasahara, T. Ohnishi, Y. Mizukami, O. Tanaka, S. Ma, K. Sugii, N. Kurita, H. Tanaka, J. Nasu, Y. Motome, T. Shibauchi, and Y. Matsuda, *Nature (London)* **559**, 227 (2018).
- [41] H. Yao and D.-H. Lee, *Phys. Rev. Lett.* **107**, 087205 (2011).
- [42] V. S. de Carvalho, H. Freire, E. Miranda, and R. G. Pereira, *Phys. Rev. B* **98**, 155105 (2018).
- [43] J. Aftergood and S. Takei, [arXiv:1910.08610](https://arxiv.org/abs/1910.08610).
- [44] T. Mizoguchi and T. Koma, *Phys. Rev. B* **99**, 184418 (2019).
- [45] H.-C. Jiang, Z.-C. Gu, X.-L. Qi, and S. Trebst, *Phys. Rev. B* **83**, 245104 (2011).
- [46] F. Trouselet, G. Khaliullin, and P. Horsch, *Phys. Rev. B* **84**, 054409 (2011).
- [47] Z. Zhu, I. Kimchi, D. N. Sheng, and L. Fu, *Phys. Rev. B* **97**, 241110(R) (2018).

- [48] M. Gohlke, R. Moessner, and F. Pollmann, *Phys. Rev. B* **98**, 014418 (2018).
- [49] N. D. Patel and N. Trivedi, *Proc. Natl. Acad. Sci. U.S.A.* **116**, 12199 (2019).
- [50] Y.-F. Jiang, T. P. Devereaux, and H.-C. Jiang, *Phys. Rev. B* **100**, 165123 (2019).
- [51] C. Hickey and S. Trebst, *Nat. Commun.* **10**, 530 (2019).
- [52] S. Liang, M.-H. Jiang, W. Chen, J.-X. Li, and Q.-H. Wang, *Phys. Rev. B* **98**, 054433 (2018).
- [53] J. S. Gordon, A. Catuneanu, E. S. Sørensen, and H.-Y. Kee, *Nat. Commun.* **10**, 2470 (2019).
- [54] K. Ido and T. Misawa, *Phys. Rev. B* **101**, 045121 (2020).
- [55] H.-Y. Lee, R. Kaneko, L. E. Chern, T. Okubo, Y. Yamaji, N. Kawashima, and Y. B. Kim, *Nat. Commun.* **11**, 1639 (2020).
- [56] T. Misawa, R. Nakai, and K. Nomura, *Phys. Rev. B* **100**, 155123 (2019).
- [57] T. Misawa and K. Nomura, *Sci. Rep.* **9**, 19659 (2019).
- [58] J. Nasu and Y. Motome, *Phys. Rev. Research* **1**, 033007 (2019).
- [59] H.-D. Chen and J. Hu, *Phys. Rev. B* **76**, 193101 (2007).
- [60] X.-Y. Feng, G.-M. Zhang, and T. Xiang, *Phys. Rev. Lett.* **98**, 087204 (2007).
- [61] H.-D. Chen and Z. Nussinov, *J. Phys. A* **41**, 075001 (2008).
- [62] A. Terai and Y. Ono, *Prog. Theor. Phys. Suppl.* **113**, 177 (1993).
- [63] Y. Hirano and Y. Ono, *J. Phys. Soc. Jpn.* **69**, 2131 (2000).
- [64] Y. Tanaka and K. Yonemitsu, *J. Phys. Soc. Jpn.* **79**, 024712 (2010).
- [65] J. Ohara and S. Yamamoto, *J. Phys. Conf. Ser.* **868**, 012013 (2017).
- [66] Y. Tanaka, M. Daira, and K. Yonemitsu, *Phys. Rev. B* **97**, 115105 (2018).
- [67] H. Seo, Y. Tanaka, and S. Ishihara, *Phys. Rev. B* **98**, 235150 (2018).
- [68] G. Baskaran, S. Mandal, and R. Shankar, *Phys. Rev. Lett.* **98**, 247201 (2007).
- [69] See the Supplemental Material at <http://link.aps.org/supplemental/10.1103/PhysRevLett.125.047204> for effects of the edge geometry and pulsed magnetic-field dependence on the spin transport.
- [70] This can be explained as follows. Since the system has the local symmetry before and after the introduction of the pulsed field, each eigenstate is specified by a set of the eigenvalues of  $\eta$  in the L region. Let us start with the initial state given as  $|\Psi; \eta_1, \eta_2 \dots\rangle$ . After the pulse at the left edge, the final state should be given within the first-order perturbation as  $|\Psi(t)\rangle = |\Psi'; \eta_1, \eta_2 \dots\rangle + A \sum_i c_i |\Phi_i; \eta_1, \eta_2 \dots - \eta_i \dots\rangle$ , where  $c_i$  is some constant and  $|\Psi'\rangle$  and  $|\Phi_i\rangle$  belong to the distinct subspaces specified by different sets of eigenvalues of  $\eta$  at the left edge. On the other hand, when some operator  $O$  commutes with  $\eta$  at the left edge,  $O|\Psi'\rangle$  belongs to the same subspace as  $|\Psi'\rangle$ . (For example,  $O$  is  $S^z$ ,  $\xi$ , or  $\eta$  in the M or R region.) Therefore, the first-order component of  $A$  in  $\langle\Psi(t)|O|\Psi(t)\rangle$  vanishes. These considerations are also confirmed numerically, which is shown in Supplemental Material [69].
- [71] Y. Singh and P. Gegenwart, *Phys. Rev. B* **82**, 064412 (2010).
- [72] Y. Singh, S. Manni, J. Reuther, T. Berlijn, R. Thomale, W. Ku, S. Trebst, and P. Gegenwart, *Phys. Rev. Lett.* **108**, 127203 (2012).
- [73] R. Comin, G. Levy, B. Ludbrook, Z.-H. Zhu, C. N. Veenstra, J. A. Rosen, Y. Singh, P. Gegenwart, D. Stricker, J. N. Hancock, D. van der Marel, I. S. Elfimov, and A. Damascelli, *Phys. Rev. Lett.* **109**, 266406 (2012).
- [74] S. K. Choi, R. Coldea, A. N. Kolmogorov, T. Lancaster, I. I. Mazin, S. J. Blundell, P. G. Radaelli, Y. Singh, P. Gegenwart, K. R. Choi, S.-W. Cheong, P. J. Baker, C. Stock, and J. Taylor, *Phys. Rev. Lett.* **108**, 127204 (2012).
- [75] T. Takayama, A. Kato, R. Dinnebier, J. Nuss, H. Kono, L. S. I. Veiga, G. Fabbri, D. Haskel, and H. Takagi, *Phys. Rev. Lett.* **114**, 077202 (2015).
- [76] K. Kitagawa, T. Takayama, Y. Matsumoto, A. Kato, R. Takano, Y. Kishimoto, S. Bette, R. Dinnebier, G. Jackeli, and H. Takagi, *Nature (London)* **554**, 341 (2018).
- [77] Y. Kajiwara, K. Harii, S. Takahashi, J.-i. Ohe, K. Uchida, M. Mizuguchi, H. Umezawa, H. Kawai, K. Ando, K. Takanashi *et al.*, *Nature (London)* **464**, 262 (2010).
- [78] C. W. Sandweg, Y. Kajiwara, A. V. Chumak, A. A. Serga, V. I. Vasyuchka, M. B. Jungfleisch, E. Saitoh, and B. Hillebrands, *Phys. Rev. Lett.* **106**, 216601 (2011).
- [79] B. Heinrich, C. Burrowes, E. Montoya, B. Kardasz, E. Girt, Y.-Y. Song, Y. Sun, and M. Wu, *Phys. Rev. Lett.* **107**, 066604 (2011).
- [80] C. Hahn, G. de Loubens, O. Klein, M. Viret, V. V. Naletov, and J. Ben Youssef, *Phys. Rev. B* **87**, 174417 (2013).
- [81] A. Kimel, A. Kirilyuk, P. Usachev, R. Pisarev, A. Balbashov, and T. Rasing, *Nature (London)* **435**, 655 (2005).
- [82] C. D. Stanciu, F. Hansteen, A. V. Kimel, A. Kirilyuk, A. Tsukamoto, A. Itoh, and T. Rasing, *Phys. Rev. Lett.* **99**, 047601 (2007).
- [83] W. K. Hiebert, A. Stankiewicz, and M. R. Freeman, *Phys. Rev. Lett.* **79**, 1134 (1997).
- [84] X. Liu, T. Berlijn, W.-G. Yin, W. Ku, A. Tsvelik, Y.-J. Kim, H. Gretarsson, Y. Singh, P. Gegenwart, and J. P. Hill, *Phys. Rev. B* **83**, 220403(R) (2011).
- [85] F. Ye, S. Chi, H. Cao, B. C. Chakoumakos, J. A. Fernandez-Baca, R. Custelcean, T. F. Qi, O. B. Korneta, and G. Cao, *Phys. Rev. B* **85**, 180403(R) (2012).
- [86] R. D. Johnson, S. C. Williams, A. A. Haghighirad, J. Singleton, V. Zapf, P. Manuel, I. I. Mazin, Y. Li, H. O. Jeschke, R. Valentí, and R. Coldea, *Phys. Rev. B* **92**, 235119 (2015).
- [87] H. B. Cao, A. Banerjee, J.-Q. Yan, C. A. Bridges, M. D. Lumsden, D. G. Mandrus, D. A. Tennant, B. C. Chakoumakos, and S. E. Nagler, *Phys. Rev. B* **93**, 134423 (2016).
- [88] F. Freund, S. Williams, R. Johnson, R. Coldea, P. Gegenwart, and A. Jesche, *Sci. Rep.* **6**, 35362 (2016).
- [89] S. C. Williams, R. D. Johnson, F. Freund, S. Choi, A. Jesche, I. Kimchi, S. Manni, A. Bombardi, P. Manuel, P. Gegenwart, and R. Coldea, *Phys. Rev. B* **93**, 195158 (2016).
- [90] S. M. Winter, Y. Li, H. O. Jeschke, and R. Valentí, *Phys. Rev. B* **93**, 214431 (2016).
- [91] D. Weber, L. M. Schoop, V. Duppel, J. M. Lippmann, J. Nuss, and B. V. Lotsch, *Nano Lett.* **16**, 3578 (2016).
- [92] M. Ziatdinov, A. Banerjee, A. Maksov, T. Berlijn, W. Zhou, H. Cao, J.-Q. Yan, C. A. Bridges, D. Mandrus, S. E. Nagler *et al.*, *Nat. Commun.* **7**, 13774 (2016).

- [93] M. Grönke, P. Schmidt, M. Valldor, S. Oswald, D. Wolf, A. Lubk, B. Büchner, and S. Hampel, *Nanoscale* **10**, 19014 (2018).
- [94] B. Zhou, Y. Wang, G. B. Osterhoudt, P. Lampen-Kelley, D. Mandrus, R. He, K. S. Burch, and E. A. Henriksen, *J. Phys. Chem. Solids* **128**, 291 (2019).
- [95] B. Zhou, J. Balgley, P. Lampen-Kelley, J.-Q. Yan, D. G. Mandrus, and E. A. Henriksen, *Phys. Rev. B* **100**, 165426 (2019).
- [96] S. Mashhadi, Y. Kim, J. Kim, D. Weber, T. Taniguchi, K. Watanabe, N. Park, B. V. Lotsch, J. H. Smet, M. Burghard *et al.*, *Nano Lett.* **19**, 4659 (2019).
- [97] E. Gerber, Y. Yao, T. A. Arias, and E.-A. Kim, *Phys. Rev. Lett.* **124**, 106804 (2020).
- [98] S. Biswas, Y. Li, S. M. Winter, J. Knolle, and R. Valentí, *Phys. Rev. Lett.* **124**, 106804 (2020).
- [99] J. G. Rau, E. K.-H. Lee, and H.-Y. Kee, *Phys. Rev. Lett.* **112**, 077204 (2014).
- [100] J. Rusnačko, D. Got-fryd, and J. Chaloupka, *Phys. Rev. B* **99**, 064425 (2019).
- [101] G. Baskaran, D. Sen, and R. Shankar, *Phys. Rev. B* **78**, 115116 (2008).
- [102] A. Koga, H. Tomishige, and J. Nasu, *J. Phys. Soc. Jpn.* **87**, 063703 (2018).
- [103] T. Minakawa, J. Nasu, and A. Koga, *Phys. Rev. B* **99**, 104408 (2019).
- [104] A. Koga, T. Minakawa, Y. Murakami, and J. Nasu, *J. Phys. Soc. Jpn.* **89**, 033701 (2020).
- [105] J. Oitmaa, A. Koga, and R. R. P. Singh, *Phys. Rev. B* **98**, 214404 (2018).
- [106] A. Koga and J. Nasu, *Phys. Rev. B* **100**, 100404(R) (2019).